Green Synthesized Silver Nanoparticles Using Argyreia Nervosa Leaf Extract and Their Antimicrobial Activity

Parvathalu K (parvathalu.k@gmail.com)
Government City College (A), Osmania University
Chinmayee S
Government City College (A), Osmania University
Preethi B
Government City College (A), Osmania University
Swetha A
Government City College (A), Osmania University
Maruthi G
Government City College (A), Osmania University
Pritam M
Michigan Technological University
Sreenivas B
Rice University-BRC
Ramu Naidu S
University of Hyderabad
Sheeba Merlin
University of Hyderabad
Murali B
University of Hyderabad
Vijay M
Government City College (A), Osmania University
Moses K
Busitema University
Chinni Krishna D
Government City College (A), Osmania University
Bala Bhaskar P
Government City College (A), Osmania University

Research Article

Keywords: Metallic Nanoparticles, Green synthesis, crystalline size, antibacterial activity

Posted Date: March 17th, 2023

DOI: https://doi.org/10.21203/rs.3.rs-2670251/v1

Additional Declarations: No competing interests reported.

Version of Record: A version of this preprint was published at Plasmonics on April 6th, 2023. See the published version at https://doi.org/10.1007/s11468-023-01835-8.

Abstract

The biogenic synthesis of silver nanoparticles (AgNPs) has attracted many researchers due to their physical, chemical, optical, and biological properties, embracing range of activities such as antibacterial, antifungal, anti-inflammatory, and anti-cancer activities. The purpose of this work is to synthesize and characterize AgNPs using Argyreia Nervosa (AN) plant leaf extract as well as to test their antimicrobial applications. In this work, silver nitrate ($AgNO_3$) at 0.1mM concentration, and stable AgNPs were synthesized and observed by monitoring the colour change of the solution from light yellow to brown. The UV-Vis spectrum shows a peak at 445nm, confirming the formation of AN-AgNPs and Fourier-transformed infrared (FTIR) results confirm the presence of chemical groups which act as reducing agents stabilizing the AN-AgNPs and antimicrobial capping agents enhancing antimicrobial properties of AN-AgNPs. The crystalline behaviour of these AN-AgNPs confirms through X-Ray Diffraction (XRD) peaks. The morphology of AN-AgNPs and their size shows different sizes, ranging from 10 to 40nm using Scanning Electron Microscopy (SEM). The disk diffusion assay shows the antimicrobial activity over *E-Coli* pathogenic microorganisms of clinical interest. The obtained results confirm a more significant antimicrobial effect of the biogenic AN-AgNPs maintaining low cytotoxicity. This work presents a potential way to produce non-toxic biogenic AgNPs with enhanced antibacterial activity, which can meet the increasing global demand for biogenic AgNPs as an alternative to antibiotics.

Introduction

The nano-material research encourages designing different types of nano-scale devices. Nanoparticles (NPs) with a size range of 1-100nm, and different shapes provide unique physical, chemical, optical properties, and biological properties[1–3]. Nanotechnology is the most used research field in translational research that integrates all disciplines of engineering and sciences. Nanotechnology has created many opportunities in all material industries such as electronics, biotechnology, healthcare, agriculture, and tissue engineering[4–6]. Metal nanoparticles have gained attention for biomedical applications due to their multi-functional properties. Extensive research has been done on silver nanoparticles (AgNPs) owing to their broad range of industrial applications such as water purification, antimicrobial, medical devices, sensors, and the food industry[7–12]. The chemical and physical methods are used in the synthesis of metal nanoparticles, but, they are capped or stabilized with hazardous chemicals[13]. Alternatively, green synthesis is the best method because of the low toxicity, low cost, eco-friendly, and easy processing[14–16]. Furthermore, plants, leaves, and fruits are easily available sources of bioactive phytochemicals such as proteins, polyphenols, flavonoids, alkaloids, amines, ketones, and aldehydes etc., which act as reducing, stabilizing, and capping agents in the process conversion of metal ions to metal nanoparticles, leading to the high production of metal nanoparticles with multifunctional properties. Among various metal nanoparticles, AgNPs have been placed as the top priority for the last two decades due to their unique applications in material, medical, and biomedical industries such as antimicrobial, anticancer, and photo-catalytic activity[17].

Plant-mediated and microorganisms are two primary sources to synthesize metal nanoparticles. Most plants have been found medically important to cure different diseases. Synthesized metal nanoparticles using plant leaf/root/fruit extracts are more advantageous than the synthesis of metal nanoparticles using microorganisms. Since, it does require complex processes such as isolation, culture maintenance, and many purification steps. With this, it has become a major focus for researchers to develop the green synthesis of metal nanoparticles using different parts of plants (leaf, peel, fruit, root, and flowers) [18–24]. The phytochemicals present in the plant extract play an important role in the process of conversion of metal ion into stable metal nanoparticles with potential applications[25–34].

Recent studies have been focused on the green synthesis of AgNPs using different plant leaves, but the biogenic of AgNPs using indigenous plant extracts exhibiting potential antibacterial and anticancer activity has not been studied to a large extent. Argyreia plant shows medicinal values such as antioxidant, antiulcer, antimicrobial, and antiviral. AN plant leaves have been used to treat diseases of the nervous system. With this knowledge of Argyreria Nervosa plant leaves (AN), the synthesized silver nanoparticles using AN plant leaves extract help to study a potential effect of antimicrobial activity.

In this work, AgNPs synthesized using AN leaves extract and AN has various phytochemical compounds that are involved in the reduction of metal ions into nanoparticles (MNP)[35–45]. The synthesized (AN-AgNPs) silver nanoparticles were characterized by using ultraviolet (UV)-Vis spectrometry, Fourier transforms infrared (FTIR), X-ray diffraction (XRD), scanning electron microscopy (SEM), and Zeta potential. The antibacterial activity of the AN-AgNP was studied using the disc diffusion method.

Materials And Methods

Materials

Argyreia nervosa leaves were obtained from a herbal garden in the Hyderabad, India. All other chemicals such as silver nitrate, acetone, were purchased from Sigma Aldrich, Bangalore, India.

Methodology

Argyreia nervosa leaves were cleaned and dried for a few days in normal sunlight. Then AN leaves were ground to make powder and 1gram of AN powder was added to 100ml water. The mixture was heated for 30 minutes at 60^0C temperature under magnetic stirring of 500rpm. 200ml silver nitrate solution with 0.1mM was prepared under magnetic stirring of 500rpm at a temperature 80^0C. Then AN extract solution was filled in the burette and added in drop wise manner to 200ml silver nitrate solution at 80^0C under 500rpm magnetic stirring. The AN-AgNPs samples were collected with different concentrations. Finally, AN-AgNPs were separated by centrifugation (5000rpm) and allowed to dry at 50 ^{0}C for further characterization process. The synthesis process is shown in Figure.1

Characterization Of An-agnps

UV spectroscopy

The UV-Vis was used to see the formation of AN-AgNPs particles. The AN-AgNPs solution was scanned over the range of 250-800nm by using a UVJASCO V-750 spectrometer.

Fourier-transform Infrared (Ftir)

The IR spectra of AN leaf aqueous extract and the centrifuged AN-AgNPs sample were used to identify the possible phytochemical and biomolecules constituents involved in the synthesis and capping of AN-AgNPs. The samples were analyzed by IR thermo Fisher Nicolet iS5. The spectra were recorded from 400 to 4000cm^{-1}.

Scanning Electron Microscopy (Sem)

FE-SEM was used to characterize the morphology and particle size of AN-AgNPs. A thin film of oven dried AN-AgNP samples was prepared and used over a carbon coated copper grid via a ZEISS Merlin Compact instrument operated at an accelerated voltage of 20kV.

Zeta Potential And Zeta Seizer

The zeta potential of particles was analysed by using the Zeta-sizer Nano-ZS. Measurements were carried out at 25°C temperature in aqueous media. The zeta potential was calculated from the electrophoretic (charge) mobility based on the Smoluchowski theory.

X-ray Diffraction

The structure of nanoparticles was analysed by using the XRD Bruker D8 Advance. The miller indices, d-spacing were calculated from the XRD data using X pert high Score software and then structure details were analysed.

Antibacterial Activity Of An-agnps On Epec By Evaluating The Disk Diffusion Method (Ddm)

To detect the antibacterial potential of green synthesised AN-AgNPs against *Enteropathogenic E. coli* (EPEC), Gentamycin is recommended to be used as one of the positive controls to test antimicrobial effect and Luria Bertani broth (LB broth) is used as the negative control. (100µl of OD 600 = 1) EPEC is plated on LB agar plates and discs coated with 50µl of AN-AgNPs are placed and incubated for 12 hours along with AN leaves extract control at 37°C. The zone of inhibition is measured by calculating the diameter of the clear zone in cm.

Results And Discussions

The focus of this study is to characterize AN-AgNPs and test antibacterial activity at different concentrations. The phytochemicals and biomolecules present in the extract could help to form active sites on the capping of metal nanoparticles. These flavonoids can donate an electron, and phenolics exhibit a chelating effect (a chemical compound that can bind tightly to metal ions) on the metal ions, which could be responsible for reducing metal ions into metal nanoparticles. The characteristics of metal nanoparticles were studied using UV-Vis, FTIR, SEM, EDX, XRD, and antibacterial activity[37].

Fourier Transform Infrared (Ftir) Spectroscopy

The FTIR spectra of the AN aqueous extract and AN-AgNPs recorded to identify the probable biomolecules and phytochemical functional groups which could be responsible for the reduction and stability of AgNPs. The phytochemical profile of AN extract aqueous shows transmission peaks at 594, 1628 and 3308 cm^{-1}, respectively (Fig. 2). The phytochemical profile of AN-AgNPs shows suppression of transmission peaks at 496, 1300, 1670, 2363 and 3308cm^{-1}. The FTIR band 3308cm^{-1} assigned to the intermolecular H bands, most probably water molecules and 1628cm^{-1} is attributed to N-H stretching in amines, and C = 0 stretching of ketones or acids. All the vibrational peaks in the AN extract spectrum were suppressed, and we observed more transmission peaks. The phenolic structure relationship plays a vital role in AN to reduce several species. The abundance of the alcohol group makes it a powerful antioxidant and a strong reducing agent for the formation of metal nanoparticles. Furthermore, the biomolecules in the plant leaves extract play a dual role of reducing and capping of formation of AgNPs.

Uv-vis Absorption Spectroscopy

The formation of AgNPs was first identified by a visual color change in $AgNO_3$ and with a control drop rate of AN extract in $AgNO_3$ solution, as time increased. The color of the mixture gradually changes from yellowish to brown confirming the formation of AN-AgNPs. This might be due to the reduction of the silver ions leading to the excitation of surface Plasmon Resonance (SPR) of the AN-AgNPs. To confirm this, The UV-Vis absorption spectra (wavelength range: 200-700nm) was recorded from each synthesized set of AN-AgNPs at different concentrations. Biogenic AN-AgNPs show the maximum absorbance at 445nm which showed stable range for AgNPs formation. The AN-AgNPs colloidal solution shows distinct peaks from 442nm to 450nm for different AgNP concentrations. It was observed that AN stabilized AgNPs colloidal solution absorption peak shifted from shorter wavelengths to longer wavelengths and it might be due to the increasing size of metal nanoparticles (Inserted in Figure.3).

Scanning Electron Microscopy

The morphological study of biogenic AN-AgNPs was investigated by field emission scanning electron microscopy (FE-SEM). Figure 4 shows the presence of spherical shape metal nanoparticles with different sizes ranging from 30 to 40 nm. The average particle size was measured to be approximately 20nm. The particle size distribution was calculated from a histogram, considering 200 particles, measured the average size using the Image-J software. The metal nanoparticles were well dispersed and not in direct contact with each other, which could be explained by the stabilizing action of capping agents present in the AN extract. This clearly shows that particles are dispersed in a homogeneous manner and play an important role in different biomedical activities. The FE-SEM confirms that the metal nanoparticles were dispersed in uniform distribution with spherical shapes of the silver nanoparticles.

Zeta Potential And Zeta Seizer

The change of Zeta potential as the function of AN-AgNPs concentration is shown in Fig. 7. The surface potential of metal nanoparticles is the potential difference between the medium where the metal nanoparticles are dispersed and the accessible surface of dispersed metal nanoparticles which can be analysed using zeta sizer. This property plays an important role to understand the surface interaction of metal nanoparticles and indicating the long-term stability of the dispersion. The Zeta potential of AN-AgNPs shows stability as the function of AN-AgNPs concentration. Figure 4 Shows zeta potential value of biosynthesized AN-AgNPs was found to be -21mV. For synthesized nanoparticles, the values of zeta potential greater than + 25 mV or less than − 25 mV have high degrees of stability. It indicates that the AN-AgNP particles show highly stable in colloidal solution.

X-ray Diffraction (Xrd) Analysis

The crystallographic nature of biogenic AN-AgNP nanoparticles was confirmed by X-Ray diffraction pattern, recorded on an Analytical X-pert high score plus MRD X-ray diffraction instrument, with Cu Kα radiation (λ = 0.15418 nm) over the processing range 2θ = 10^0–90^0, with a step of 0.02 degree. The XRD pattern of bio-synthesized AN-AgNPs (Fig. 5), shows several peaks. The XRD data of the synthesized AgNPs, show different peaks, where the four main peaks are located at 38^0, 44.3^0, 64^0, and 77.2^0, corresponding to the (111), (200), (220), and (311) reflection planes, respectively to the structure of face-cantered cubic (FCC) crystal of silver (JCPDS, No. 04-0783). In addition to Braggs peaks for silver nano-crystal, additional peaks were observed at 16.9^0, 29.6^0, and 33.6^0. The presence of these additional peaks might be due to AN extract which contains biomolecules that could help the reduction of silver ions and stabilization of silver nanoparticles. On the basis of Bragg's diffraction angle (θ) and the full width of half maximum (β) for more intense peaks (111) corresponding average crystalline size was calculated as 22.2nm. The average size of the crystalline was calculated based on the Debye-Scherrer equation. The details of lattice parameters, cell volume, and crystalline size are mentioned in Table.1.

Table.1. Crystalline parameters for different planes

S.NO	Planes (hkl)	2θ	Sinθ	Cosθ	FWHM(β) Radians	Interplanar Spacing(d)	Lattice Constant(a)	Cell Volume(a^3)	Crystalline Size(D)
1	111	38	0.35	0.95	0.0065	2.39	4.11	69.42	23
2	200	44.3	0.38	0.92	0.0042	2.07	4.12	69.93	35
3	220	64	0.53	0.85	0.0076	1.46	4.13	70.44	22
4	311	77.2	0.62	0.78	0.006	341.	4.10	68.92	30

The size of the crystaaline GT-AgNPs was calculated using the Debye-Scherrer formula.

$$\text{Crystallin e size (D)} = \frac{0.9\lambda}{\beta Cos\theta}$$

Where λ is the X-ray wavelength (0.1546nm), β is the full width of half maximum (FWHM) (line broadening at half maximum) in radians, θ is the Bragg's angle. Crystalline size for all planes is mentioned in Table.1.

Antibacterial Activity

The antimicrobial activity of the aqueous AN plant's leaf extract and biogenic AN-AgNPs was carried out by the disc diffusion method against pathogenic organism *E-Coli, Luria Bertani broth (negative control), and Gentamycin* (positive control) as shown in Fig. 5. AN-AgNPs showed higher antibacterial activity in terms of zone of inhibition against *E-Coli* when compared to the aqueous leaf extract of *AN*. The zone of inhibition was observed 11mm for all concentration of AN-AgNPs within the error bars against *E-Coli* and this concentration of AN-AgNP is efficient enough to remove bacteria colony. The aqueous leaf extract did not show antibacterial activity. The zone of inhibition on bacterial strain was measured after 12 h of incubation at 37°C. The zone of inhibition on bacterial strain is shown in Fig. 7 as the function AN-AgNPs concentration.

Conclusions

In this work, the green synthesis of silver nanoparticles from AN plant's leaf extract was observed under UV-Vis spectroscopy at 445nm and FTIR spectroscopy identifies the biomolecules involved in the reduction of Ag^+ ions to Ag-nanoparticles. The crystallinity nature of silver nanoparticles was confirmed using XRD study. AgNPs are found to be very effective to act as an anti-bacterial agent. However, there must experiments be carried out to find the evaluation of efficacy on animals as well as human beings. As these nanoparticles are non-toxic and safe in vivo studies, the green synthesized silver nanoparticles can be used for the treatment of different diseases. The antibacterial activity of prepared AN-AgNPs was evaluated using disc diffusion assay and AN-AgNPs showed potential antibacterial activity against the Enteropathogenic *E. Coli* bacteria strain. Our findings open one potential path to produce biogenic AgNPs, to meet

the increasing global demand for their applications as an alternative to antibiotics. However, further research on AN-AgNPs is needed to explore their potential applications in bio-nano-medical technology.

Declarations

Data Availability Statement

The authors are going to provide data of any specific analysis

Author Contributions

The first and corresponding author collected and analysed data. The other authors helped in discussion of project at various levels.

Funding declaration

Thank you to Commissionerate of Collegiate Education, Telangana, India for providing funding support.

Conflicts of interest

"There are no conflicts to declare".

Acknowledgements

The Authors would like to thanks to department of chemistry, department of biochemistry, University of Hyderabad, Government City College (A), Hyderabad, Telangana for providing facilities.

References

1. Shenton, W, Douglas, T, Young, M, Stubbs, G, and Mann, S. Adv. Mater. 1999, 11, 23–256;
2. Tang, S., Mao, C., Liu, Y., Kelly, D. Q., and Banerjee, S. K. IEEE Trans, 2007;
3. Thakkar, K., Mhatre, S., and Parikh, R. Nanotechnol. Biol. Med.2009 6, 257 – 62;
4. S. Fakhari, M. Jamzad and H. Kabiri Fard, Green Chem. Lett. Rev., 2019, 12, 19 – 2;
5. Ramsden,.J.Nanotechnology:William Andrew, 2016;
6. S. Ahmed, M. Ahmad, B. Swami and S. Ikram, J. Adv. Res., 2016, 7, 17–28;
7. Tang, S., Mao, C., Liu, Y., Kelly, D. Q., and Banerjee, S. K. IEEE Trans, 2007;
8. Thakkar, K., Mhatre, S., and Parikh, R. Nanotechnol. Biol. Med.2009, 6, 257–62;
9. Chen, H., Roco, M. C., Li, X. & Lin, Y. Trends in nanotechnology patents. Nat. Nanotechnol, 2008, 3, 123–125.
10. Chen, H., Roco, M. C., Li, X. & Lin, Y. Trends in nanotechnology patents. Nat. Nanotechnol,2008, 3, 123–125;
11. Smetana, A. B., Klabunde, K. J. & Sorensen, C. M. J. Colloid Interface Sci.,2005, 284, 521–526;
12. Lee, H., Chou, K. S. & Huang, K. C. Nanotechnology, 2005, 16, 2436–2441;
13. Shenton, W, Douglas, T, Young, M, Stubbs, G, and Mann, S. Adv. Mater. 1999,11, 23–256;
14. Wakuda, D., Kim, K. S. & Suganuma, K. Scripta Mater, 2008, 59,649–652;
15. Anna, Z, Eva,S., Adriana.Z., Maria.G.,Jan, H., Procedia Chem.2009, 1, 1560–1566;
16. Kholoud, M. M, Abou.E,Ala. A,Abdulrhman, Reda.A.A.A.,Arab. J. Chem. 2010, 3, 135–140;
17. Haggag, E. G.; Elshamy, A. M.; Rabeh, M. A.; Gabr, N. M.; Salem, M.; Youssif, K. A.; Samir, A.; Bin Muhsinah, A.; Alsayari, A.; Abdelmohsen, U. R. Int. J. Nanomed. 2019, 14, 6217–6229.
18. Iravani, S. Green Chem. 2011, 13, 2638–2650;
19. Duan, H; Wang, D; Li, Y., Chem. Soc. Rev. 2015, 44, 5778–5792;
20. V. Kumar and S. Anthony, Surf. Chem. Nanobiomater. 2016, 265–300;
21. Hasan, S. Res. J. Recent Sci, 2015, 4, 1–3;
22. Prabu, H. J. & Johnson, I. Karbala, 2015, Int. J. Mod. Sci. 1, 237–246;

23. Shakeel, A. H, Saifullah, M.A,Babulal,S,Saiqa.I, J. Radiat. Res. Appl. Sci.2016, 9, 1–7;
24. Khatoon,A,H,Farheen.K,Nabeel.A,Sibhghatulla.S,Syed.M,Danish.R,Shazi,S,Mohammad,H,A,Adel,M,Ahmed,A,Hayatul,I,Danish,I,Rajiv,D, Life Sci. 2018, 15, 430–434.
25. Annu,Shakell,A,Gurpreet,K,Praveen,S,Sandeep, S,Saiqa, I, J. Appl. Biomed. 2018, 16, 221–231.
26. Padalia, H., Moteriya, P. & Chanda, S. Arab. J Chem. 2015, 8, 732–741;
27. Lakshmanan, G., Sathiyaseelan, A., Kalaichelvan, P. T. & Murugesan, K. Karbala Int. J. Mod. Sci.2018, 4, 61–68.
28. Benakashani, F., Allafchian, A. & Jalali, S. A. H. Green Chem. Lett. Rev. 2017, 10, 324–330;
29. D. A. Kumar, V. Palanichamyand S. M. Roopan, Spectrochim. Acta, Part A, 2014, 127, 168–171;
30. R. Sankar, P. Manikandan, V. Malarvizhi, T. Fathima, K. S. Shivashangariand V. Ravikumar,Spectrochim. Acta, Part A, 2014, 121, 746–750;
31. V. Dhand, L. Soumya, S. Bharadwaj, S. Chakra, D. Bhattand B. Sreedhar, Mater. Sci. Eng., C, 2016, 58, 36–43;
32. A. S. Saifullah, M. Ahmad, B. L. Swamiand S. Ikram, J. Radiat. Res. Appl. Sci.,2016, 9, 1–7;
33. M. M. Khalil, E. H. Ismail, K. Z. El-Baghdadyand D. Mohamed, Arabian J. Chem.,2014, 7, 1131–1139;
34. F. Ameen, S. AlYahya, M. Govarthanan, N. ALjahdali, N. Al-Enazi, K. Alsamhary, W. A. Alshehri, S.S. Alwakeeland S. A. Alharbi, J. Mol. Struct.,2020, 1202, 1272;
35. P. Kalakonda, Nanomaterials and Nanotechnology,2016, 6, 1847980416663672;
36. P. Kalakonda, S.Banne, Plasmonics, 2017, 12 (4), 1221;
37. P. Kalakonda, S. Banne, Plasmonics, 2018, 13(4), 1265;
38. K. Parveen, V. Banse and L. Ledwani, AIP Conf. Proc., 2016, 1724, 020048;
39. S. K. Nune, N. Chanda, R. Shukla, K. Katti, R. R. Kulkarni, S. Thilakavathyand K. V. Katti, J. Mater.Chem.,2009, 19, 2912–2920;
40. Widatalla, H. A., Yassin, L. F., Alrasheid, A. A., Ahmed, S. A. R., Widdatallah, M. O., Eltilib, S. H., & Mohamed, A. A. 2022, 4(3), 911–915;
41. Sriramprabha, R.; Divagar, M.; Ponpandian, N.; Viswanathan, C.. J.Electrochem. Soc. 2018, 165, 498-B507
42. S. Tangand J. Zheng, Adv. Healthcare Mater.,2018, 7, 1701503;
43. B. Le Ouayand F. Stellacci, Nano Today,2015, 10, 339–354;
44. A. K. Keshari, R. Srivastava, P. Singh, V. B. Yadavand G. Nath, J. Ayurveda Integr. Med.,2020, 11, 37–44;
45. H. Gandhiand, S. Khan, J. Nanomed. Nanotechnol.,2016, 7, 1000366;

Figures

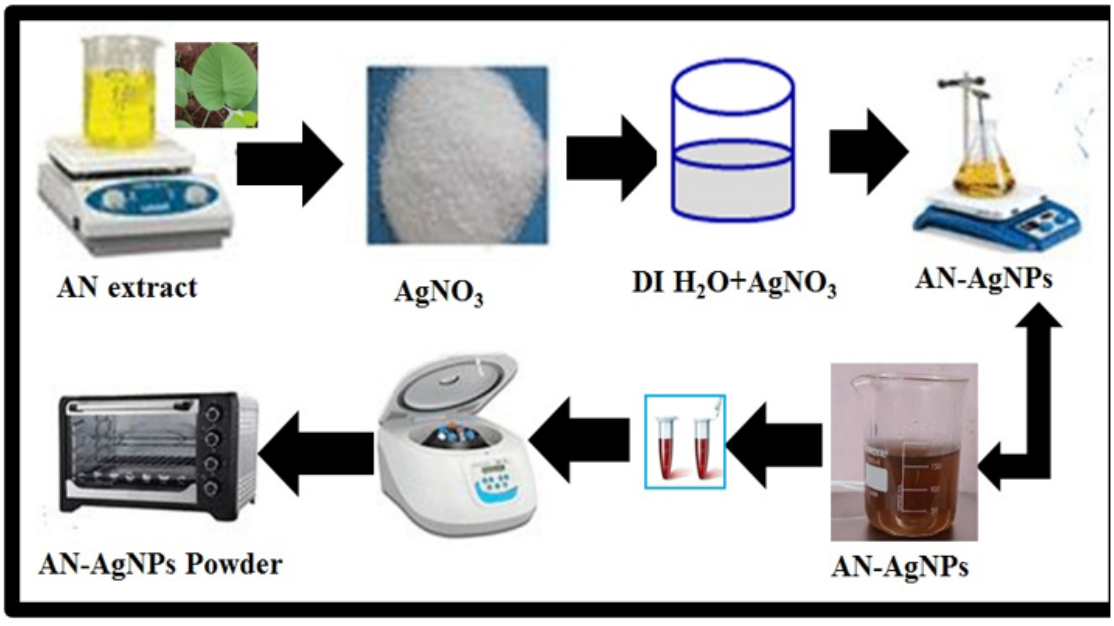

Figure 1

Green synthesis process of AN-AgNPs

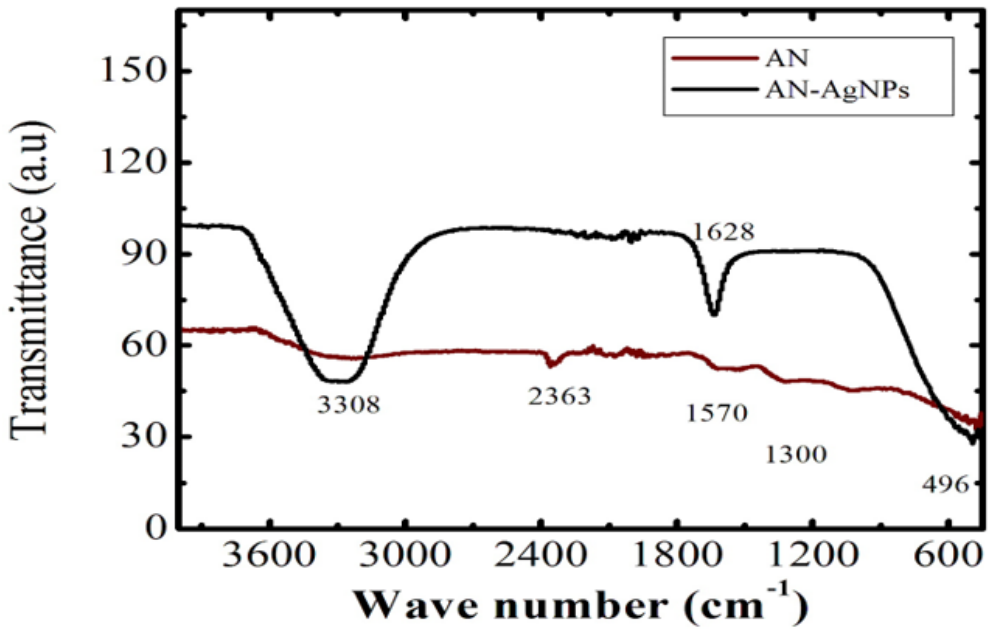

Figure 2

FTIR spectrum of AN and AN-AgNPs

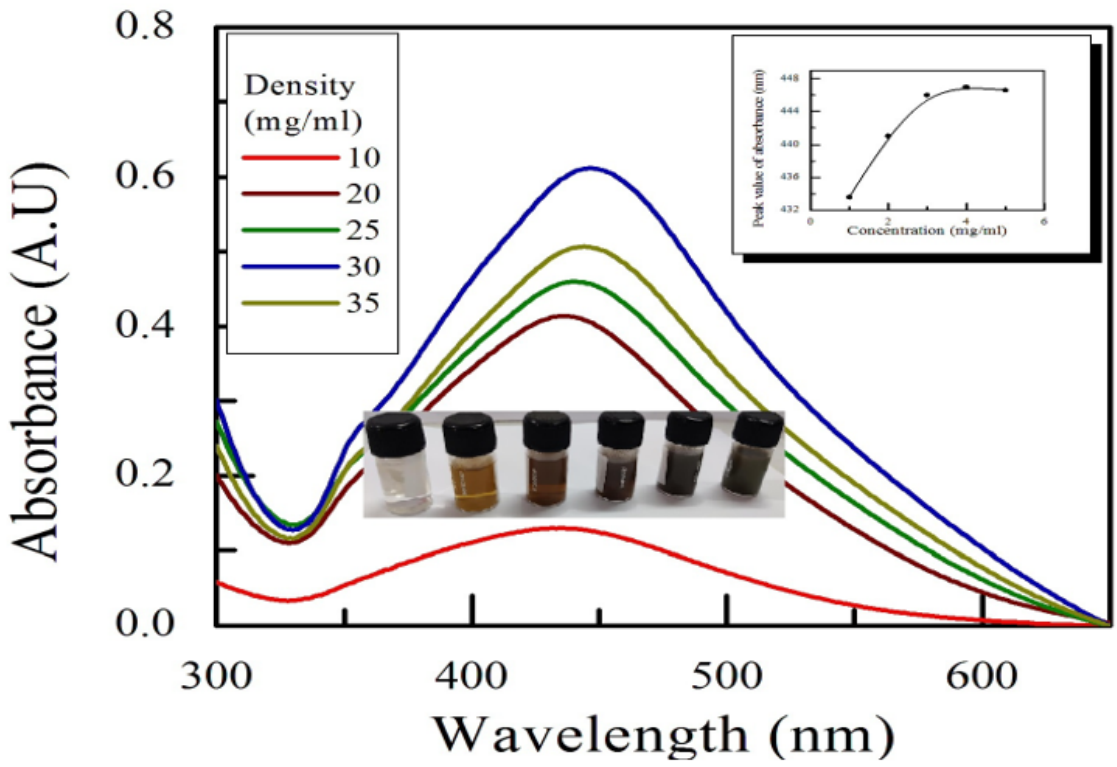

Figure 3

UV spectrum of AN-AgNPs

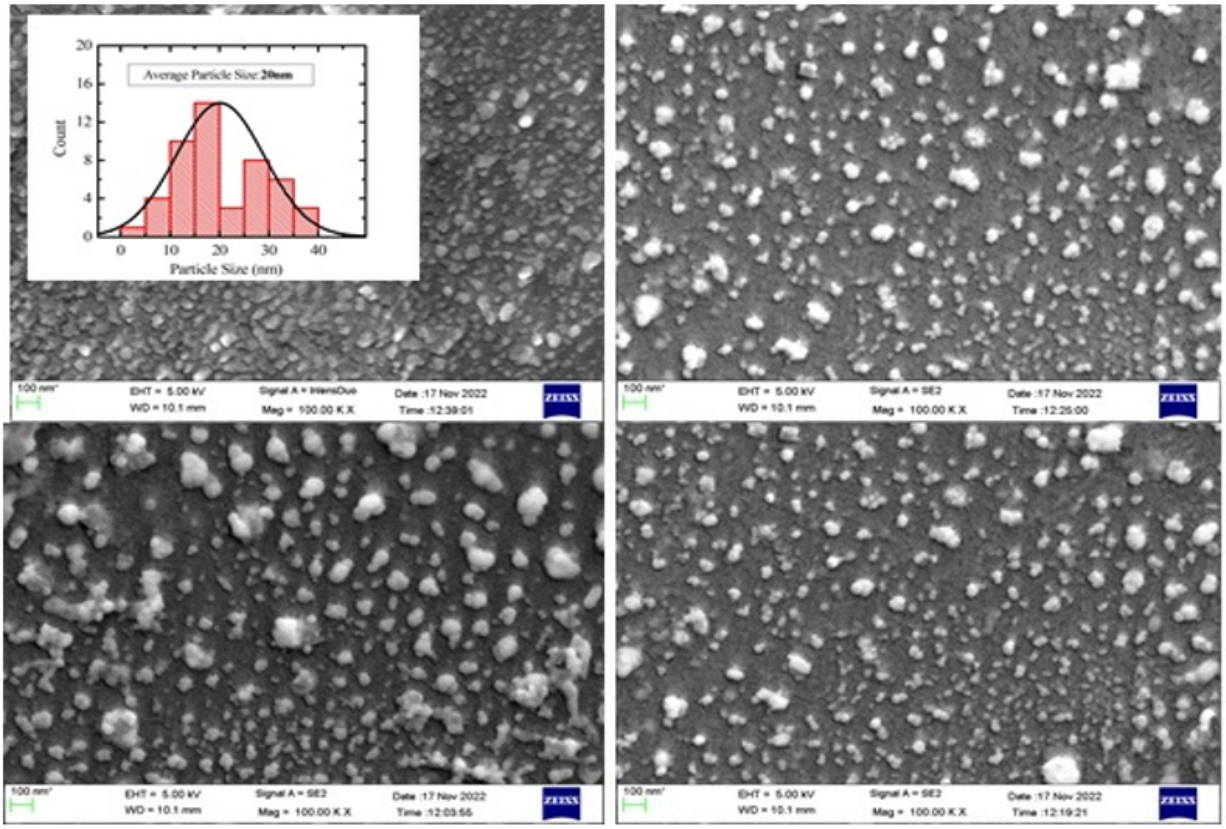

Figure 4

Fig.3.SEM images of AN-AgNPs

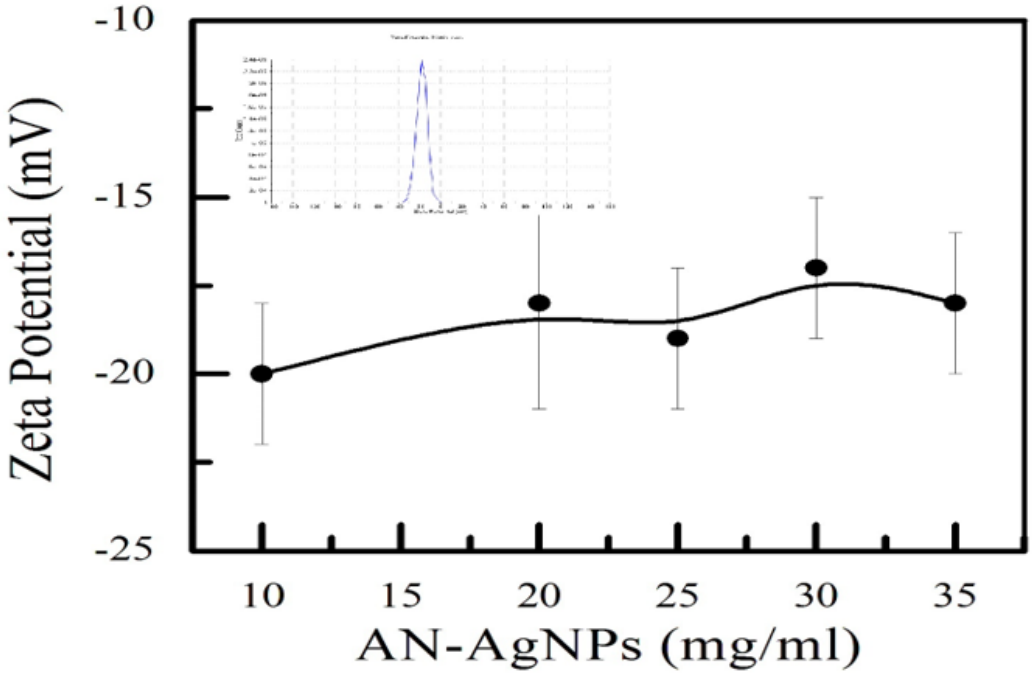

Figure 5

Fig. 4 Variation of Zeta potential as the function of GT-AgNPs

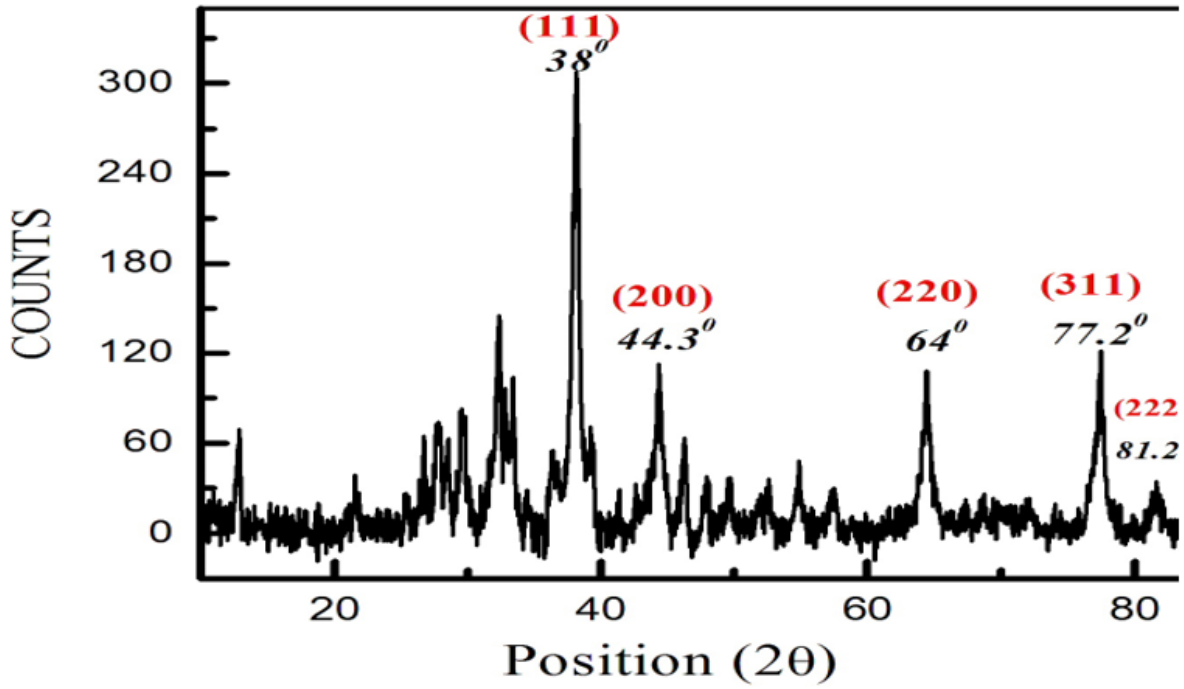

Figure 6

Fig.5 XRD pattern of AN-AgNPs: Face centered cubic (FCC) crystal structure of silver

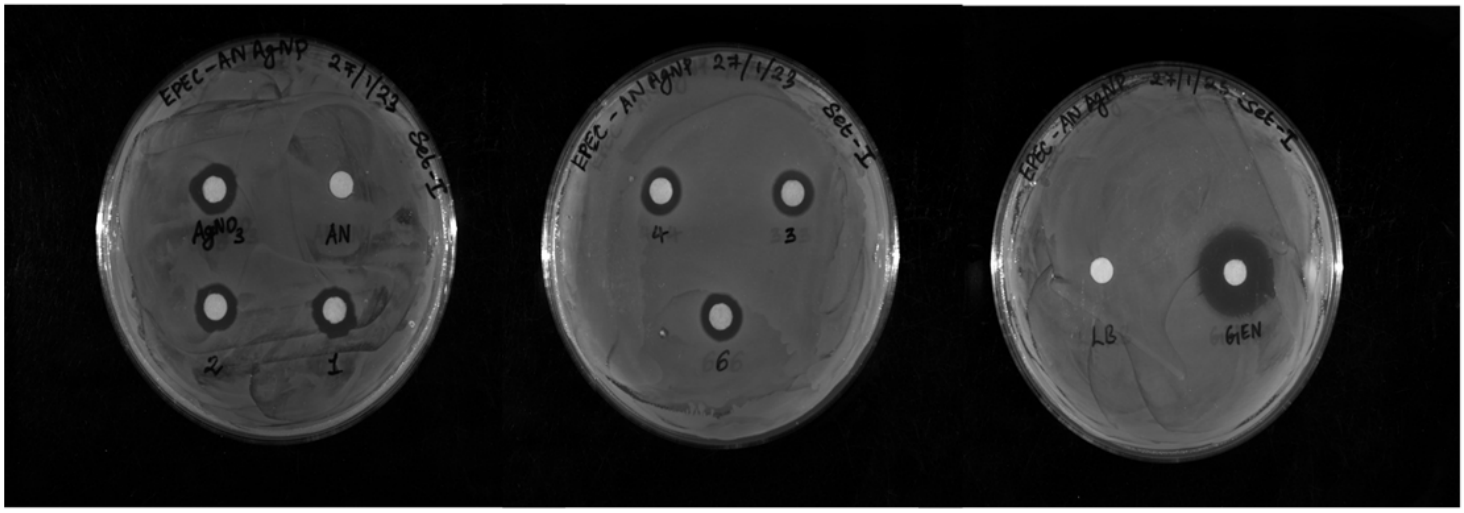

Figure 7

Fig.6. Antimicrobial susceptibility conducted through disk diffusion method. Zones of inhibition of different concentrations of biogenic AN-AgNPs showed against *E. coli*, AN extract, LB broth (negative control), and Gentamicin (positive control).

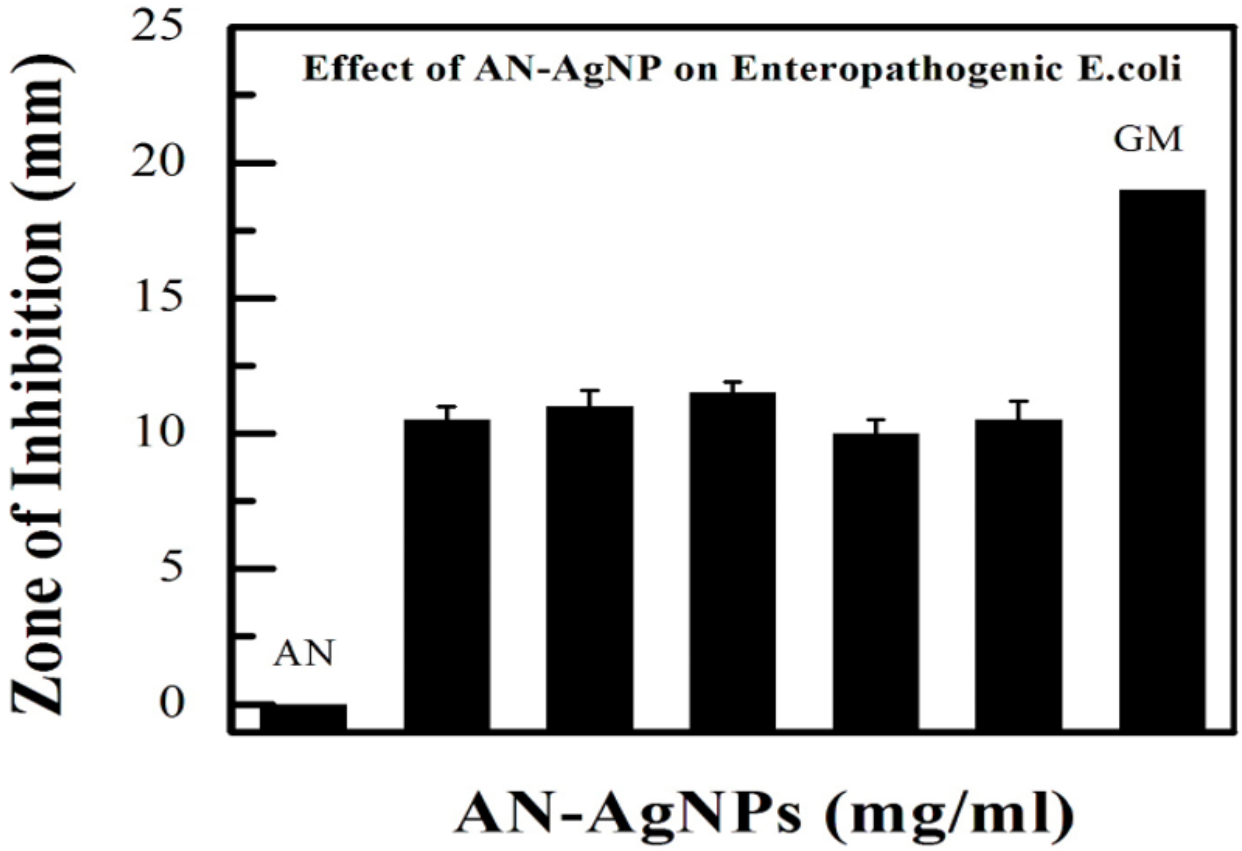

Figure 8

Fig.7. Zones of inhibition is the function of concentrations of biogenic AN-AgNPs against *E. coli*